The Two-Domain Structure of 5′-Adenylylsulfate (APS) Reductase from *Enteromorpha intestinalis* Is a Requirement for Efficient APS Reductase Activity†

Sung-Kun Kim,‡,§ Varinnia Gomes,‡,|| Yu Gao,||,⊥ Kala Chandramouli,# Michael K. Johnson,# David B. Knaff,§ and Thomas Leustek*,||

Department of Chemistry and Biochemistry and Center for Biotechnology and Genomics, Texas Tech University, Lubbock, Texas 79409-1061, Biotechnology Center for Agriculture and the Environment, Department of Plant Biology and Pathology, Rutgers University, New Brunswick, New Jersey 08901-8520, and Department of Chemistry and Center for Metalloenzyme Studies, University of Georgia, Athens, Georgia 30602

Received September 12, 2006; Revised Manuscript Received November 7, 2006

ABSTRACT: 5′-Adenylylsulfate (APS) reductase from *Enteromorpha intestinalis* (EiAPR) is composed of two domains that function together to reduce APS to sulfite. The carboxyl-terminal domain functions as a glutaredoxin that mediates the transfer of electrons from glutathione to the APS reduction site on the amino-terminal domain. To study the basis for the interdomain interaction, a heterologous system was constructed in which the C domain of EiAPR was fused to the carboxyl terminus of the APS reductase from *Pseudomonas aeruginosa* (PaAPR), an enzyme that normally uses thioredoxin as an electron donor and is incapable of using glutathione for this function. The hybrid enzyme, which retains the [4Fe−4S] cluster from PaAPR, was found to use both thioredoxin and glutathione as an electron donor for APS reduction. The ability to use glutathione was enhanced by the addition of Na_2SO_4 to the reaction buffer, a property that the hybrid enzyme shares with EiAPR. When the C domain was added as a separate component, it was much less efficient in conferring PaAPR with the ability to use glutathione as an electron donor, despite the fact that the separately expressed C domain functioned in two activities that are typical for glutaredoxins, hydroxyethyl disulfide reduction and electron donation to ribonucleotide reductase. These results suggest that the physical connection of the reductase and C domain on a single polypeptide is critical for the electron-transfer reaction. Moreover, the effect of Na_2SO_4 suggests that a water-ordering component of the reaction milieu is critical for the catalytic function of plant-type APS reductases by promoting the interdomain interaction.

Sulfur reduction by sulfate-assimilating organisms proceeds through two sequential electron-transfer reactions. The first is a two-electron reduction, catalyzed by one of several different but related types of sulfonucleotide reductases that produce sulfite from sulfate. The second is the six-electron reduction of sulfite to sulfide, catalyzed by sulfite reductase. The currently known assimilatory sulfonucleotide reductases are structurally and mechanistically diverse enzymes that all share a common ancestry. The first member of this family of enzymes to be characterized is CysH from *Escherichia coli* (*1*). This enzyme reduces 3′-phospho-5′-adenylylsulfate (PAPS) using thioredoxin (Trx)[1] or glutaredoxin (Grx) as an electron donor, and it is characteristic of the PAPS-dependent, assimilatory sulfonucleotide reductases in diverse eubacteria, archaea, fungi, and one example from moss (*2*, *3*). Another member of this family, from *Pseudomonas aeruginosa* (PaAPR), also uses Trx as an electron donor, but it reduces 5′-adenylylsulfate (APS) rather than PAPS (*4*). PaAPR has extensive amino acid sequence homology with CysH, including a conserved active-site Cys, but differs structurally from CysH by the presence of a $[4Fe-4S]^{2+}$ center and four additional conserved Cys residues. Two different models have been proposed for the role of the Cys in PaAPR. One postulates that all four Cys residues serve as ligands to the cluster irons (*5*), and another postulates that only three of these Cys residues serve as cluster ligands (*6*). PaAPR is characteristic of the APS-utilizing assimilatory sulfonucleotide reductase from diverse eubacteria and archaea (*7*). A recently discovered example of an iron−sulfur cluster-containing-type sulfonucleotide reductase from *Bacillus subtilis* shows sequence and structural characteristics that places it in the same group as PaAPR; however, it is able to reduce both APS and PAPS (*8*). A third type of sulfonucle-

† This work was supported by a grant from the U.S. Department of Agriculture (Grant 2002−35318-12503 to T.L. and D.B.K.) and the National Institutes of Health (GM62542 to M.K.J.).

* To whom correspondence should be addressed: Rutgers University, Biotech Center, 59 Dudley Road, New Brunswick, NJ 08901-8520. Telephone: (732) 932-8165. Fax: (732) 932-8165. E-mail: leustek@aesop.rutgers.edu.

‡ These authors contributed equally to this work.

§ Texas Tech University.

|| Rutgers University.

⊥ Current address: Corning Incorporated, 2 Alfred Road, Kennebunk, Maine 04043.

University of Georgia.

[1] Abbreviations: APS, 5′-adenylylsulfate; EiAPR, *Enteromorpha intestinalis* APS reductase; hAPR, hybrid APS reductase; PaAPR, *Pseudomonas aeruginosa* APS reductase; Grx, glutaredoxin; GR, glutathione reductase; Trx, thioredoxin; TR, thioredoxin reductase; GSH, reduced glutathione; MALDI−TOF, matrix-assisted laser desorption ionization−time of flight; mBBr, monobromobimane; SDS−PAGE, sodium dodecyl sulfate−polyacrylamide gel electrophoresis.

10.1021/bi0618971 CCC: $37.00
Published on Web 12/16/2006

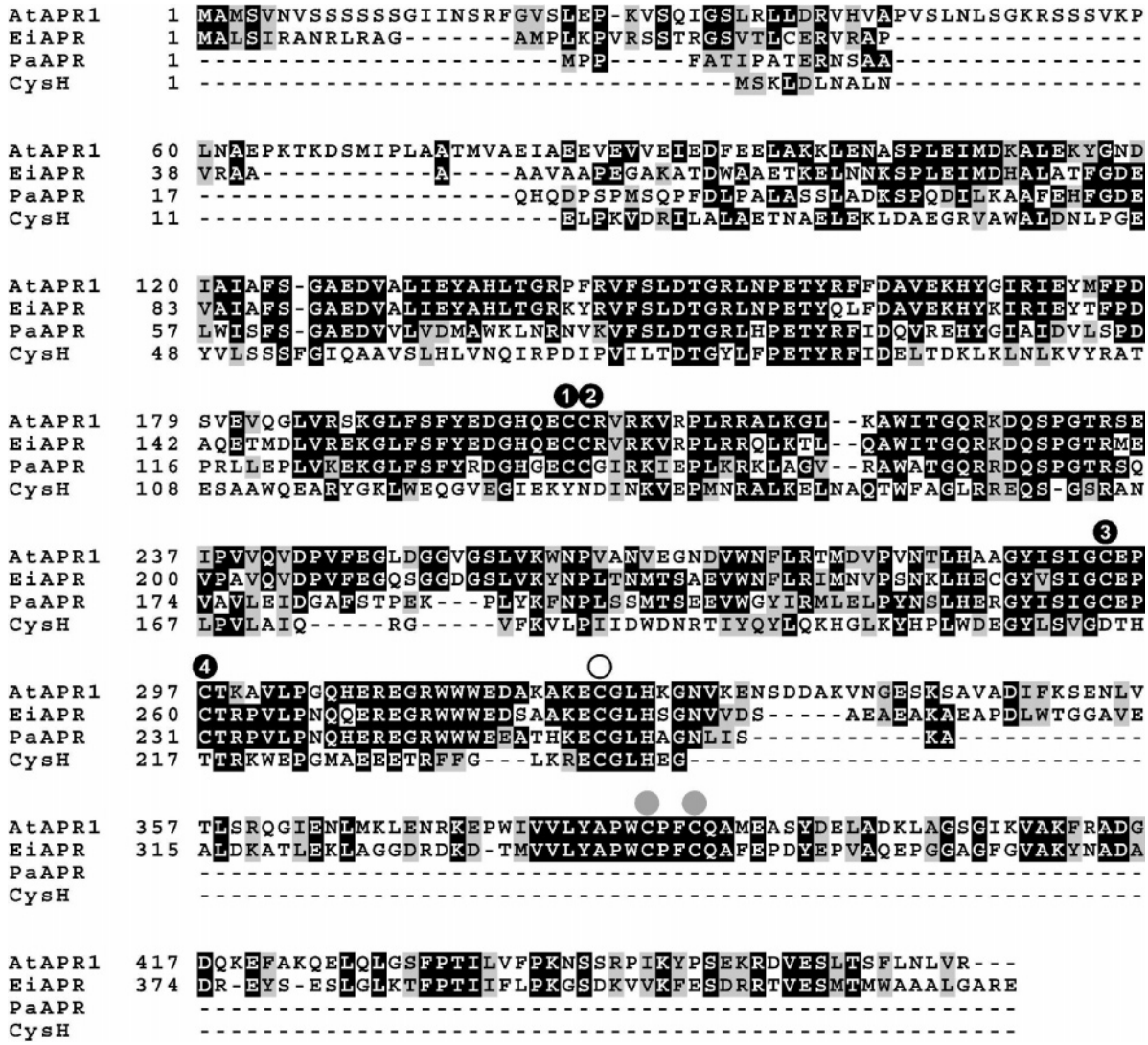

FIGURE 1: Primary structure of plant- and bacterial-type assimilatory APS reductases. A sequence alignment was created with *Arabidopsis* APR1 (NP_192370), EiAPR (AAC26855), PaAPR (NP_250447), and *E. coli* CysH (NP_417242) (GenBank accession numbers in parentheses) using the ClustalW function of MegAlign version 5.07. The diagram was created with BoxShade (http://www.ch.embnet.org/software/BOX_form.html). Amino acid residues found in 50% of the sequences are boxed in black, and similar amino acids are boxed in gray. Conserved Cys residues in the plant APS reductases and PaAPR that have been proposed to be ligands to the $[4Fe-4S]^{2+}$ center are indicated by black circles numbered 1−4. An alternate hypothesis is that only three of these Cys residues ligate the cluster (see the Introduction for the description). The active-site Cys is indicated with a white circle, and the C-domain Cys residues proposed to function as the glutaredoxin active site are indicated by gray circles.

otide reductase, characteristic of the enzyme from plants (*9*−*11*), is the APS reductase from *Enteromorpha intenstinalis* (EiAPR) (*12*). This enzyme contains a $[4Fe-4S]^{2+}$ cluster, and it shows high amino acid sequence homology to PaAPR within a domain that is proximal to the amino terminus (*13*). In addition, it contains a domain proximal to the C terminus with homology to Trx that is not found in CysH or PaAPR. In the related APS reductase from *Arabidopsis thaliana*, the C-proximal domain was shown to confer the ability of the enzyme to use glutathione (GSH) as an electron donor (*14*), suggesting that it functions as a Grx and not a Trx. A protein alignment showing the domain structure of EiAPR compared with PaAPR is shown in Figure 1. As references, the sequences of the *Arabidopsis* APR and *E. coli* CysH were also included. EiAPR and PaAPR sequences are 52% identical, and the proteins have very similar calculated isoelectric points (PaAPR, 6.26; EiAPR, 6.91).

The reaction mechanism of the sulfonucleotide reductases is incompletely understood and may be expected to vary in the different types, owing to the diversity of structures that exist. CysH displayed kinetic properties that indicated that it undergoes a Ping-Pong-type catalytic reaction (*1*). It was proposed that Trx reduces a disulfide formed between two active-site Cys residues, one contributed by each of two subunits of the dimeric enzyme. Then, the reduced enzyme transfers the stored electrons to PAPS to release sulfite. Kinetic studies demonstrated that PaAPR also exhibited kinetic properties indicative of a Ping-Pong-type mechanism, although a complete kinetic analysis was not performed (*4*). This information, in combination with site-directed mutagenesis and thiol quantitation measurements (*6*), led to a proposed mechanism in which the active-site Cys residue of PaAPR (i.e., the residue that corresponds to the single active-site Cys present in *E. coli* CysH) forms part of an intramolecular disulfide when the enzyme is oxidized and it is this disulfide that is the target of reduction by Trx. An alternative mechanism was more recently proposed that argues against the presence of an intramolecular disulfide

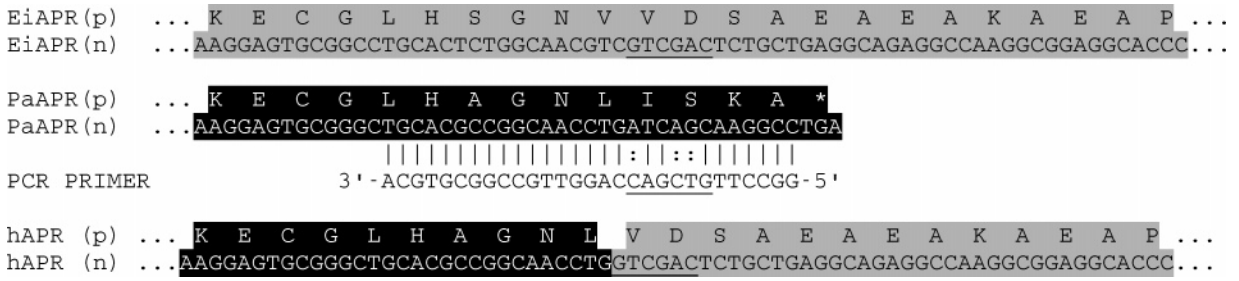

FIGURE 2: Construction of a hybrid protein composed of the PaAPR sequence linked with the C domain of EiAPR. The strategy utilized a unique *Sal*I site at the junction between the reductase and C-terminal domain of *Ei*APR. A *Sal*I site was introduced into the PaAPR coding sequence by PCR using a primer with mismatched bases indicated in the figure (base pairs are indicated with a vertical line, and mismatches are indicated with a colon). The resulting PCR fragment was cloned into pET-EiAPR (*12*), replacing the EiAPR reductase domain with PaAPR. The protein (p) and nucleotide (n) sequences are shown for the junction between the reductase and C domain in EiAPR (black letters and gray shading), the 3′ end of the PaAPR coding sequence (white letters and black shading), and the junction of the hybrid between the PaAPR and EiAPR C domain. All sequences in the diagram are aligned.

bond in PaAPR and, furthermore, proposes that Trx reduction occurs in a later, rather than an earlier, step in the catalytic cycle (*5*, *15*). Nonetheless, both models propose that a transient, disulfide-linked intermediate is formed between Trx and PaAPR. This intermediate was experimentally demonstrated by identification of a covalently bound, intermolecular disulfide between the active-site Cys of PaAPR and one of the active-site Cys of Trx (*16*). Other studies have identified the active-site Cys functioning as the acceptor of a sulfur-transfer reaction from APS that forms a sulfonate suggestive of a reaction intermediate (*5*, *17*). Further studies will be required to determine the sequence of electron-transfer reactions and the role of the iron−sulfur center, in the assimilatory APS reductases.

The function of the two-domain structure of the plant-type APS reductase has been of keen interest since the discovery of this enzyme type. To date, there are several examples of enzymes that have a fused domain structure with Trx or Grx (*18*−*20*). All of the known plant and algal APS reductases (deduced from nucleotide sequences present in the molecular databases) have this two-domain structure, suggesting that it is present in all chloroplast-containing species and may be an adaptation to the milieu of the chloroplast stroma where this enzyme is localized. The C domain was hypothesized to play a role in either catalysis or the regulation of activity (*9*). Subsequent studies showed that the C domain of one of the *A. thaliana* enzyme isoforms functions as a Grx and that the efficiency of APS reduction is greatest when the C domain is located on the same polypeptide as the reductase domain. Specifically, catalytic efficiency is markedly reduced when the reductase and C domains, expressed as separate proteins, are mixed in an APS reductase assay (*14*). The fact that the reductase domain of this *A. thaliana* enzyme retains some ability to catalyze APS reduction, albeit at a low rate, in the absence of the C domain and that the C domain alone has no ability to reduce APS demonstrates the presence of the catalytic center on the reductase domain (*14*, *17*, *21*). Trx can replace the C domain, although inefficiently, and to date, no form of Trx has been shown to function efficiently as an electron donor to the plant-type APS reductase. The C domain of this *A. thaliana* enzyme, when expressed as a separate protein, shows a number of properties typical of Grx's. It efficiently reduces cystine, hydroxyethyldisulfide, dehydroascorbate, insulin, and ribonucleotide reductase (*14*, *21*). A number of questions remain about the two-domain structure of plant-type APS reductases and the function of the C domain. Because Trx is used as a redox cofactor by bacterial APS and PAPS reductases and Trx also plays a central role in chloroplast metabolism, it is not obvious why plant APS reductases evolved a C domain that presumably freed sulfate reduction from the Trx-based electron-transport system within the chloroplast. Also of interest are the mechanistic properties of the fused-domain plant enzymes compared with the bicomponent system (e.g., PaAPR and Trx) that exists in prokaryotes. The mechanism by which the reductase and C domains interact during APS reduction is another area of interest.

To understand the structural framework that allows the two domains of the plant-type APS reductase to interact, the function of the C domain of EiAPR was studied in the context of a heterologous system. The C domain of EiAPR was tested in a reaction with PaAPR either in a free form or as a translational fusion with PaAPR. The results showed that the EiAPR C domain is able to confer GSH dependence onto PaAPR and that the efficiency of the interaction is markedly increased when the EiAPR C domain is fused to PaAPR. Interestingly, the GSH-dependent activity of the PaAPR/EiAPR C-domain fusion was enhanced by incorporation of Na_2SO_4 into the reaction buffer. Plant-type APS reductases are known to require Na_2SO_4 or other osmotic agents (kosmotropes) for activity (*9*, *22*, *23*). These results show that the interaction of the C domain and PaAPR is dependent upon the juxtaposition of the two proteins through a physical connection and the presence of water-structuring agents in the enzyme milieu. These are likely to be the same constraints that determine the interaction of reductase and C domains in their native context.

MATERIALS AND METHODS

Plasmids for Recombinant Protein Expression. Plasmids had previously been constructed for the expression of EiAPR (pET30-EAPR) (*12*), the C domain of EiAPR (pET-EiCdomain) (*13*), and PaAPR (pET-PaAPR) (*4*).

A plasmid was construction for the expression of a hybrid protein consisting of PaAPR linked to the C domain of EiAPR. The engineering strategy is depicted in Figure 2. A segment from pET-PaAPR was polymerase chain reaction (PCR)-amplified using a forward primer spanning the unique *Bgl*II site of the vector (5′-AGCACATGGACAGCCCA-GATCTGGGTA-3′, restriction site underlined) coupled with

a primer homologous with the 3′ end of the PaAPR coding sequence with three mismatched nucleotides that introduced a *Sal*I restriction site (5′-GGCCTTGTCGACCAGGTTGC-CGGCGTGCA-3′, restriction site underlined). This primer is depicted in Figure 2. The fragment was cloned into the *Bgl*II and *Sal*I sites of pET-EiAPR, replacing the coding sequence of the EiAPR reductase domain with the PaAPR coding sequence. The hybrid construction was completely sequenced and confirmed not to carry any unintended mutations.

Recombinant Protein Expression and Purification. A culture of the *E. coli* host harboring the expression plasmid was grown in LB medium containing 50 μg/mL kanamycin and 34 μg/mL chloramphenicol at 37 °C to an optical density at 600 nm of 0.6. Isopropyl-β-D-thiogalactopyranoside (IPTG) was then added, to a final concentration of 1 mM, and growth was continued for 4 h in LB medium at 30 °C. Cells were then harvested by centrifugation, resuspended in 30 mM Tris-HCl buffer (pH 8.0), passed twice through a French press at 18 000 psi, and centrifuged. The supernatant was filtered through a 0.45 μm pore-size membrane and applied to a Ni^{2+}-affinity column (HiTrap Chelating HP, obtained from Amersham Biosciences), incorporated into a BioCAD perfusion chromatography system (PerSeptive Bio-Sciences, Framingham, MA). The column was washed with 200 mL of 30 mM Tris-HCl buffer (pH 8.0) containing 500 mM NaCl (buffer A), supplemented with 25 mM imidazole. The His-tagged recombinant protein was then eluted at about 100 mM imidazole with a gradient from 25 to 250 mM imidazole. All solutions used for the Ni^{2+}-affinity chromatography were degassed and purged with helium gas. The imidazole was removed by buffer exchange against 30 mM Tris-HCl buffer (pH 8.0) containing 100 mM sodium sulfate, using an Amicon YM10 membrane. The typical yield was approximately 5 mg of protein from 1 L of culture. The protein concentration was determined by the Bradford method (*24*) using bovine serum albumin (BSA) as a standard. The protein purity and molecular mass were determined by denaturing sodium dodecyl sulfate−polyacrylamide gel electrophoresis (SDS−PAGE) and matrix-assisted laser desorption ionization−time of flight (MALDI−TOF) mass spectrometry as described previously (*6*). Absorbance spectra were measured using a Shimadzu UV-2401 PC spectrophotometer at 1.0 nm spectral resolution.

Enzyme Assays. The reagents used for enzyme assays were purchased from Sigma-Aldrich, Inc. (St. Louis, MO), thioredoxin reductase (T7915), glutathione reductase (G3364), cytidine 5′-diphosphate (C9755), 2-hydroxyethyl disulfide (380474), ATP (A3377), NADPH (N750-S); Promega, Inc. (Madison WI), thioredoxin (Z7051); Calbiochem, Inc. (San Diego, CA), glutathione (3541); Perkin-Elmer (Wellesley, MA), [^{35}S]PAPS (NEG010100UC); and Roche Molecular Biochemicals (Mannheim, Germany), nuclease P1 (236225). *E. coli* glutaredoxin derived from *grxA* (Grx) was prepared as described by Bick et al. (*14*). *E. coli* ribonucleotide reductase was the kind gift of Dr. Joanne Stubbe (Massachusetts Institute of Technology, Cambridge, MA).

APS reductase assays were carried out in 0.1 mL reactions containing 50 mM Tris-HCl (pH 8.3), 1 mM ethylenediaminetetraacetic acid (EDTA), 25.0 μM AP^{35}S (~500 Bq nmol^{-1}), the reductant system, and an enzyme using the $^{35}SO_2$ distillation method and AP^{35}S preparation method described previously (*9*). Reductant systems were varied as indicated in the figure and table captions. The reductant systems were of the following compositions: 90 μM Trx, 300 μM NADPH, and 6 units of thioredoxin reductase (TR) or 5 mM GSH, 300 μM NADPH, and 1 unit of GR. Na_2SO_4 was added to some assays at the indicated concentration. Reactions were incubated at 30 °C. The incubation time was varied depending upon the assay.

The hydroxyethydisulfide (HED) assay was in a 1 mL reaction containing 100 mM Tris-HCl (pH 8.3), 1.5 mM EDTA, 500 μM GSH, 400 μM HED, 350 μM NADPH, and 3.2 units of GR. The assay was initiated by the addition of HED and incubated at 24 °C. NADPH oxidation was monitored continuously at 340 nm using a Beckman DU-640 spectrophotometer.

Ribonucleotide reductase was assayed in a 0.4 mL reaction containing 30 mM Hepes-KOH (pH 7.6), 1.5 mM EDTA, 10 mM $MgCl_2$, 1.6 mM ATP, 1 mM CDP, 0.5 mg mL^{-1} BSA, 0.35 mM NADPH, and 0.1 μM ribonucleotide reductase with the following reductant systems: 15 μM Trx and 1 unit of TR or 2.5 mM GSH and 4 units of GR, with either Grx or C domain as indicated. The assay was initiated by the addition of CDP. Before the assay of activity, ribonucleotide reductase was reduced by incubating with 5 mM dithiothreitol (DTT) on ice for 1 h and then removed from the DTT by filtration using a Biomax centrifugal filter 10 kDa cutoff (Millipore, Inc., Bedford, MA). The assays were incubated at 24 °C, and NADPH oxidation was monitored continuously at 340 nm using a Beckman DU-640 spectrophotometer.

In all cases, the data presented are the mean of between three and six replicates, with the variation given as the standard deviation. Kinetic constants were calculated from substrate titration curves using nonlinear regression analysis with the GraphPad Prism 4.03 (GraphPad Software, Inc.).

Redox Titrations. Oxidation−reduction titrations of disulfide/dithiol redox couples were carried out as described previously (*25*, *26*) using thiol labeling with monobromobimane (mBBr), followed by quantitation of the fluorescence arising from the mBBr adducts of the protein (fluorescence was measured using an Aminco-Bowman Series 2 luminescence spectrometer, with both excitation and emission monochromators set at 1.0 nm spectral resolution). Oxidation−reduction equilibration was carried out in redox buffers consisting of defined mixtures of either oxidized and reduced DTT or oxidized glutathione (GSSG) and GSH, depending upon the E_h range being investigated, as described previously (*27*). All of the titration data gave excellent fits to the Nernst equation for a two-electron couple. E_m values were independent of the redox equilibration time (over the range from 2.0 to 2.5 h) and the total DTT or total GSH concentrations present in the redox equilibration buffer (over the range from 2.0 to 5.0 mM). Identical titration curves were observed regardless of whether the titrations were carried out under ambient oxygen concentrations or under an argon atmosphere.

Iron−Sulfur Cluster Content. The total iron content was determined according to the procedure of Massey (*28*), using ferric ammonium sulfate as a standard. Acid-labile sulfide was determined as described previously, using spinach ferredoxin as a standard (*29*). The values reported for both iron and sulfide contents represent the average of three

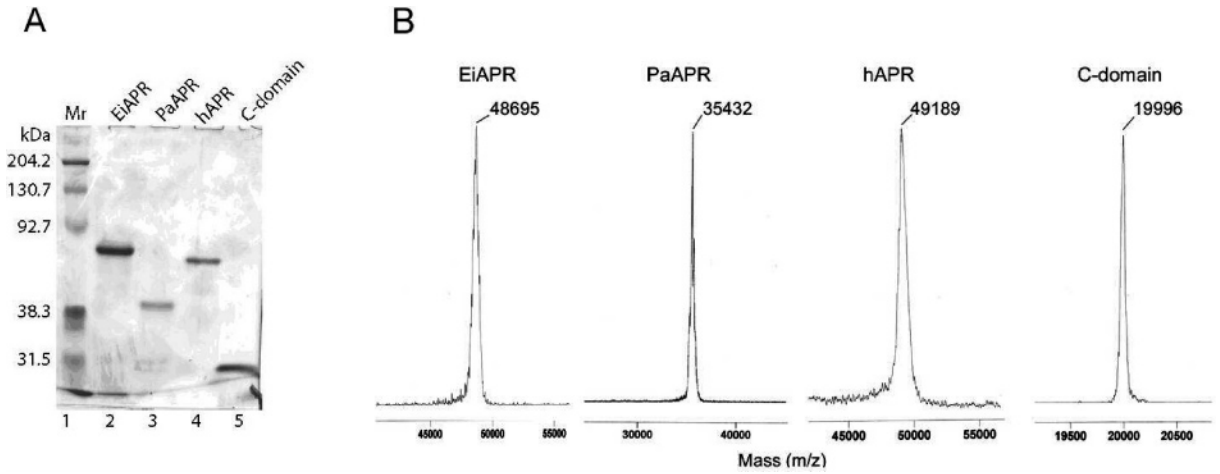

FIGURE 3: (A) SDS−PAGE of the APR proteins used in the study. Molecular-weight markers (Mr) are shown on the left (lane 1). A total of 1 μg of the indicated proteins (lanes 2−5) was analyzed by SDS−PAGE on a gel produced with 10% (w/v) acrylamide, and the proteins were detected with Coomassie Blue. The proteins were preincubated with 2-mercaptoethanol to ensure reductive cleavage of disulfide bonds. (B) MALDI−TOF mass spectrometry of the APR proteins used in the study.

replicate determinations. Resonance Raman spectra of the iron−sulfur clusters of PaAPR and hAPR were obtained as described previously (*6*) using 457 nm laser excitation.

RESULTS

To assess the function of the C domain of plant APS reductase in a heterologous system, the C domain was expressed as a free protein or as a fusion with the carboxyl terminus of PaAPR (hybrid APS reductase, hAPR). The cloning positioned the C domain to a location in PaAPR precisely analogous to its native context in EiAPR (Figure 2). The cloning also replaced the last four codons of PaAPR with the homologous codons from EiAPR. The hybrid was constructed in pET30 to place a His tag at the N terminus of the hAPR. The resulting protein was expressed in *E. coli* and purified by Ni^{2+}-affinity chromatography. hAPR and the other proteins used in this study, including recombinant EiAPR, PaAPR, and the C domain of EiAPR, were analyzed by SDS−PAGE and Coomassie Blue staining. Figure 3 shows that all of the proteins used in this study were nearly homogeneous. The electrophoresis experiment of Figure 3A was carried out under reducing conditions (i.e., in the presence of 2-mercaptoethanol), but essentially identical results were obtained in the absence of 2-mercaptoethanol (data not shown). Figure 3B shows MALDI−TOF mass spectra of these same four proteins. The experimental molecular masses (35 432 Da for PaAPR, 48 695 Da for EiAPR, 49 179 Da for hAPR, and 19 996 Da for the C-terminal domain of EiAPR) correspond, within the experimental uncertainties in the measurements, to the calculated molecular masses as $[M + H]^+$ for these proteins (35 443 Da for PaAPR, 48 708 Da for EiAPR, 49 180 Da for hAPR, and 20 003 Da for the C-terminal domain of EiAPR). The apparent molecular masses that were calculated for these four proteins from their migration, compared to the migration of molecular-mass standards, during SDS−PAGE, all differed significantly from the calculated and MALDI−TOF mass spectrometry values. The reasons for the anomalous behavior of the proteins during SDS−PAGE (under both reducing and nonreducing conditions) were not further investigated.

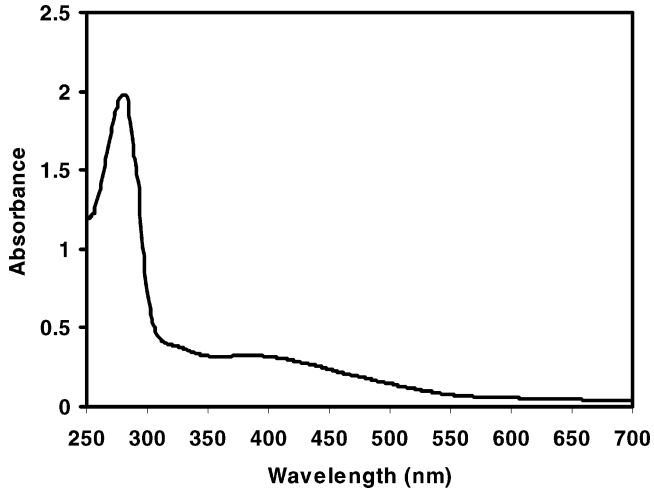

FIGURE 4: Absorbance spectrum of hAPR. hAPR was present at a concentration of 20 μM in 30 mM Tris-HCl (pH 8.0) containing 100 mM sodium sulfate.

Figure 4 shows the UV/vis absorbance spectrum of hAPR. The spectrum in the visible region, which is quite similar to that obtained previously for PaAPR, contained a broad peak with a maximum at 386 nm. It had previously been demonstrated that PaAPR contains a single $[4Fe-4S]^{2+}$ cluster that gives rise to this absorbance feature (*6*) and, because hAPR contains the entire PaAPR moiety, one would expect that this cluster would also be present in hAPR. Analysis of hAPR gave values of 3.8 ± 0.8 mol of Fe/mol of protein and 3.4 ± 0.2 mol of sulfide/mol of protein, consistent with the presence of one $[4Fe-4S]^{2+}$ cluster in the chimeric hAPR. The ratio of the absorbance at 386 nm to that at 280 nm is 0.16. The fact that this value is slightly smaller than the ratio of 0.18 found for PaAPR itself (*6*) is probably due to the presence of three tryptophan residues present in the EiAPR C-terminal domain portion of hAPR. It should be pointed out that the visible-region spectrum of EiAPR is quite similar to that shown for hAPR in Figure 4 and to the spectrum of PaAPR. However, because hAPR does not contain the region of EiAPR that binds the $[4Fe-4S]^{2+}$ cluster of the algal protein, the cluster present in hAPR can be assigned to its PaAPR domain. These results suggest that

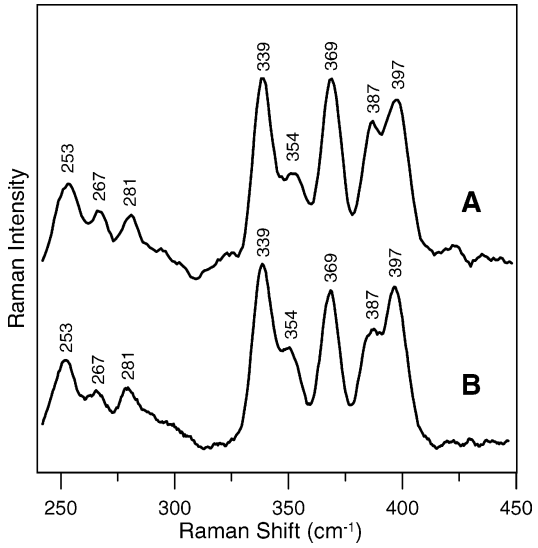

FIGURE 5: Resonance Raman spectra of PaAPR and hARP fusion proteins in the Fe−S stretching region. (A) PaAPR. (B) hAPR. The spectra were recorded at 17 K using a 457.9 nm excitation with samples that were ~2 mM in protein concentration in 100 mM Tris buffer (pH 8.0) containing 100 mM Na_2SO_4. Each spectrum is the sum of 100 scans, with each scan involving photon counting for 1 s at 1 cm^{-1} increments with 8 cm^{-1} spectral resolution.

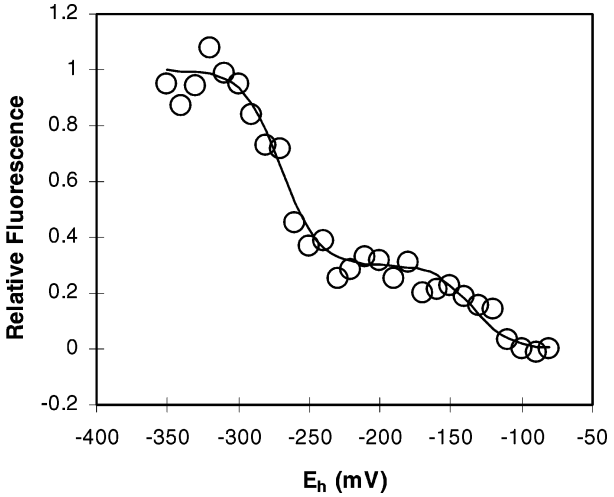

FIGURE 6: Oxidation−reduction titration of hAPR. During the 2.5 h redox equilibration phase of the titration, hAPR was present at a concentration of 1.0 μM in 100 mM Hepes-KOH buffer (pH 7.0). The redox equilibration buffer contained either a total DTT concentration of 2.0 mM (at E_h values from −250 to −350 mV) or a total GSH concentration of 2.0 mM (at E_h values from −80 to −240 mV).

fusion of the C domain of EiAPR did not markedly alter the structure of PaAPR, at least insofar as the environment of the iron−sulfur cluster is concerned. This conclusion was tested in more detail using resonance Raman spectroscopy, a technique that is sensitive to the geometry and environment of the iron−sulfur cluster (*30*). Figure 5 shows resonance Raman spectra of PaAPR and hAPR, both obtained under the same experimental conditions. The two spectra are essentially identical, showing that fusion of the C domain of EiAPR does not alter the geometry or environment of the PaAPR $[4Fe-4S]^{2+}$ cluster in any way and indicating that the C domain does not contribute to the ligation or biogenesis of the [4Fe−4S] cluster.

We had previously shown that PaAPR contains one titratable disulfide/dithiol couple (Cys140/Cys256 in the PaAPR sequence) with an E_m value of −300 mV at pH 7.0 (*6*). We had also shown that EiAPR contains two titratable disulfide/dithiol couples and that one of them (Cys342/Cys345 in the EiAPR sequence), with an E_m value of −140 mV at pH 7.0, is present in the C-terminal domain of the protein that forms part of hAPR (*13*). If both of these features are retained in the hAPR fusion, then one would expect titrations of hAPR at pH 7.0 to show two titratable disulfide/dithiols couples, one with an E_m value close to −300 mV and the other with an E_m value close to −140 mV. Figure 6 shows an oxidation−reduction titration (carried out at pH 7.0) of hAPR, using the thiol-specific reagent mBBr to monitor the thiol content as the ambient potential (E_h) is varied. As predicted, two separate two-electron couples are present, one with an $E_m = -275$ mV and one with an $E_m = -130$ mV. Average E_m values (from three titrations) were -285 ± 10 and -135 ± 10 mV, respectively. Thus, as predicted, hAPR contains two titratable disulfide/dithiol couples. Furthermore, the E_m values measured for these two couples present in hAPR are identical, within the experimental uncertainties of the measurements, to the E_m values found for these same couples when present in either PaAPR alone or EiAPR. It should be mentioned that EiAPR contains a second titratable disulfide/dithiol couple with an E_m value at pH 7.0 of −290 mV, very close to the −300 mV E_m value of the PaAPR couple. However, because neither Cys165 nor Cys285 (the two EiAPR cysteine residues that give rise to this low-potential disulfide) are present in hAPR, we can assign the low-potential components of hAPR as originating from its PaAPR portion.

Table 1: Kinetic Constants of PaAPR and hAPR Using Trx as an Electron Donor[a]

kinetic constant	PaAPR	hAPR
V_{max} (μmol min^{-1} mg^{-1})	3.7 ± 0.5	2.5 ± 0.3
$K_{m[Trx]}$ (μM)	54 ± 20	54 ± 11
$K_{m[APS]}$ (μM)	11.4 ± 3.3	7.0 ± 4.1

[a] Reaction conditions were as described in the Materials and Methods using the Trx, TR, and NADPH reductant system and without Na_2SO_4 added to the assay mixture.

After the iron−sulfur content and redox properties of hAPR were characterized, the kinetic characteristics of the fusion protein were then studied. The first step in the analysis of the kinetic properties of hAPR involved measuring the ability of the fusion protein to catalyze APS reduction using a system that generates reduced Trx (i.e., Trx, TR, and NADPH) as the electron donor (i.e., conditions that yield high activity for the reduction of APS catalyzed by PaAPR but no activity with full-length EiAPR). These experiments, carried out under initial velocity conditions, showed typical Michaelis−Menten kinetics (not shown). The results in Table 1 demonstrate that hAPR exhibits kinetic parameters under these conditions that are very similar to those characteristic of PaAPR. Although V_{max} for hAPR was approximately 68% of that observed with PaAPR, the apparent K_m values for Trx and APS were found to be similar for both enzymes. The kinetic constants measured for PaAPR in these experiments were also very similar to those previously reported (*4*, *16*). The results indicate that fusion of the EiAPR C domain to the carboxyl terminus of PaAPR did not distort its ability to catalyze Trx-dependent APS reduction.

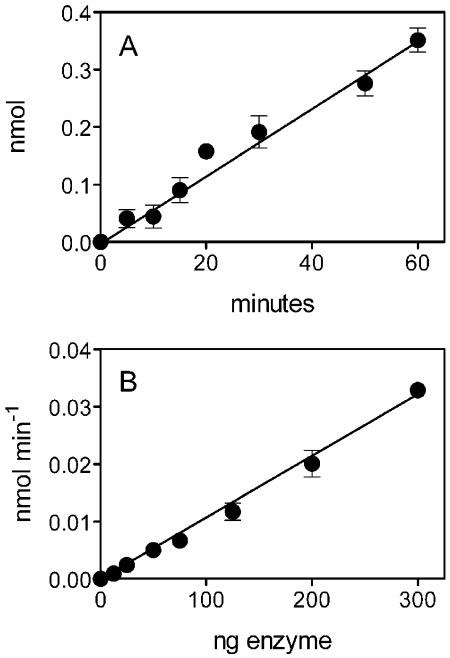

FIGURE 7: hAPR activity using GSH as an electron donor. Graph A shows a time course of APS reductase activity, and graph B shows the relationship between the reaction rate and the amount of protein added. Reaction conditions were as described in the Materials and Methods using GSH, GR, and NADPH as the reductant system and with 500 mM Na_2SO_4 added. For the time course, 50 ng of hAPR was used, and for the protein titration, the reactions were incubated for 20 min. Each data point represents the mean of at least three independent measurements. For those points without visible error bars, the standard deviation was less than the diameter of the line symbol.

Next, hAPR was tested for the ability to catalyze GSH-dependent APS reduction. The reaction conditions were those optimized for EiAPR, including the use of GSH as a reductant and the incorporation of 500 mM Na_2SO_4 in the reaction buffer. EiAPR and other plant APS reductases are well-known to show enhanced activity in the presence of Na_2SO_4. Under these reaction conditions, PaAPR has previously been shown to be completely devoid of APS reductase activity because it is unable to use reduced glutathione as an electron donor (*4*). Indeed, when either PaAPR or the C domain of EiAPR was assayed under the conditions outlined above, neither showed any detectable APS reductase activity (not shown). The data presented in Figure 7 indicate that hAPR is able to catalyze GSH-dependent APS reduction with a rate that is linear with time up to 60 min (Figure 7A). In addition, the rate of the reaction was directly proportional to the amount of enzyme added to the reaction up to 0.3 μg (Figure 7B). No activity was observed if GSH were omitted. These results indicate that fusion of the EiAPR C domain conferred PaAPR with a new activity, the ability to catalyze GSH-dependent APS reduction. These data further underscore the function of the C domain of EiAPR in mediating the interaction of plant-type APS reductases with GSH.

To further analyze the catalytic ability of hAPR, its kinetic properties were compared directly to those of EiAPR under initial velocity conditions. hAPR showed typical Michaelis−Menten kinetics when the APS or GSH concentration was varied with the cosubstrate at the saturating level. The data in Table 2 show that hAPR and EiAPR have very similar apparent K_m values for both GSH and APS. The K_m for APS

Table 2: Kinetic Constants of EiAPR and hAPR Using GSH as an Electron Donor[a]

kinetic constant	EiAPR	hAPR
V_{max} (μmol min^{-1} mg^{-1})	1.3 ± 0.2	0.15 ± 0.03
$K_{m[GSH]}$ (μM)	0.20 ± 0.06	0.03 ± 0.01
$K_{m[APS]}$ (μM)	11.0 ± 3.0	4.4 ± 2.5

[a] Reaction conditions were as described in the Materials and Methods using the GSH, GR, and NADPH reductant system and with 500 mM Na_2SO_4 added to the assay.

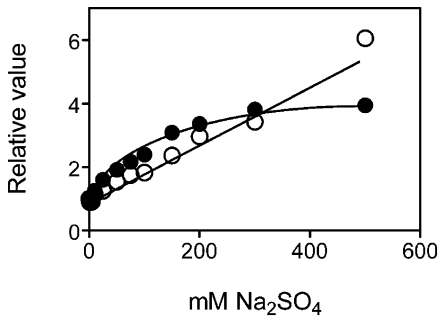

FIGURE 8: Effect of sodium sulfate on APS reductase activity. The activity of (●) EiAPR and (○) hAPR was assayed at different Na_2SO_4 concentrations. The data points are given as values relative to the activity with no Na_2SO_4 added, which was assigned a value of 1. The assay was carried out with GSH as the reductant. The data are a representative example from at least three independent experiments.

obtained for EiAPR in the current study is similar to the previously reported value, but the K_m for GSH is 7-fold lower than previously reported (*12*). The reason for this difference was not examined further. However, one possibility is that the earlier results were obtained with GSH alone as the electron donor, in contrast to the present experiments that maintained the level of GSH with GR and NADPH. GSSG could have influenced the K_m determinations, because GSSG has been shown to inactivate other forms of plant APS reductase (*31*).

A comparison of the kinetic properties of hAPR under assay conditions optimized for PaAPR and EiAPR shows that the K_m for APS is nearly the same when measured under the different conditions (Table 1 versus Table 2). However, the V_{max} using GSH as a reductant was only 6% of the value using reduced Trx as the electron donor. This indicates that, although the C domain of EiAPR is able to confer GSH dependence to PaAPR, it does not completely replace Trx, as would perhaps be expected for such a heterologous system.

Given that the activity of plant-type APS reductases is stimulated by high ionic strength, it was of interest to determine how hAPR responds to Na_2SO_4. Figure 8 shows that the GSH-dependent activity of hAPR is stimulated by Na_2SO_4. In the current experiment, the activity increased approximately linearly up to 500 mM without reaching a maximum. EiAPR activity was stimulated approximately 4-fold, with a maximum activity reached at 300−500 mM Na_2SO_4. This result indicates that the interaction of the C domain with the reductase domain or with PaAPR in the context of hAPR is enhanced by Na_2SO_4. Significantly, Na_2SO_4 did not stimulate hAPR measured with Trx as the electron donor nor did it inhibit activity (data not shown), further indicating that the Na_2SO_4 effect is specific for activity that involves the C domain.

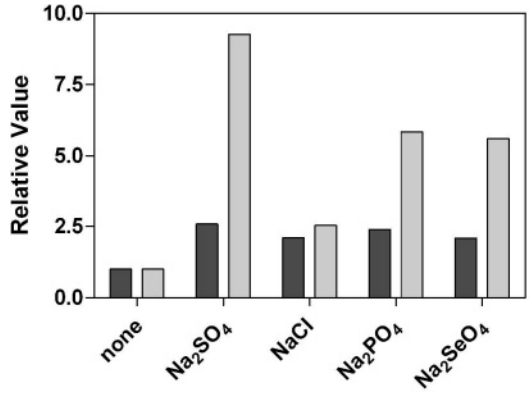

FIGURE 9: Effect of salts on APS reductase activity. EiAPR (black bars) and hAPR (gray bars) were assayed with the indicated salts present at a concentration of 500 mM. The results are presented as relative to the activity without added salt, which was assigned a value of 1. The data are a representative example from at least three independent experiments.

The basis for the stimulation of APS reductase activity by Na_2SO_4 was examined by assessing the response of EiAPR and hAPR to different salts. Na_2SO_4 is recognized as an efficient kosmotrope, an agent that effectively organizes the structure of water. When Na_2SO_4 is added to protein solutions, it stabilizes protein hydrophobic domains (*32*). A wide range of kosmotropic agents were tested, but only NaCl, Na_2PO_4, and Na_2SeO_4 were found to reproducibly stimulate the activity of EiAPR and hAPR (Figure 9). Other kosmotropic agents that had little effect on the activity included glycerol, proline, trehalose, betaine, and albumin. These results suggest that there may be a specific effect of ionic agents on APS reductase.

An important question about the GSH-dependent activity of hAPR is whether it is necessary for the C domain to be fused to PaAPR or whether the free form of the C domain could serve an electron donor for free PaAPR. In preliminary experiments, no GSH-dependent activity could be detected by assaying PaAPR activity with reduced C domain. However, when the reaction conditions were manipulated, a low but experimentally reproducible activity was observed when PaAPR was supplied with the reduced EiAPR C domain as the sole electron donor. The specific activity of 3.5 nmol min^{-1} mg^{-1} observed for this reaction was only ca. 2% of the activity observed for hAPR using GSH as the electron donor (with 500 mM Na_2SO_4; the activity was not measured in the absence of Na_2SO_4) and only 0.1% of the activity of PaAPR using reduced Trx as the electron donor. This result is presented in Figure 10, showing the affect of varying amounts of the C domain on the activity, using two different levels of PaAPR. The concentration of the C domain needed to achieve saturation of PaAPR was approximately a 44-fold molar excess of the C domain over PaAPR. Because the ratio of PaAPR to the C domain in the context of hAPR is 1, the data of Figure 10 indicate that the C domain is a very inefficient electron donor unless it is fused to the carboxyl terminus of PaAPR. One possible explanation might be that the recombinant C domain is a poor Grx, owing to the His tag or some other feature of the construction. To test this possibility, the activity of the C domain was tested in the HED reduction assay. *E. coli* Grx 1 efficiently reduce HED to the monothiol form using GSH as an electron donor. The results in Table 3 show that the EiAPR C domain is more efficient than Grx 1 in HED reduction. PaAPR itself is devoid of HED reductase activity, indicating that the HED reductase activity of hAPR is due to the C domain.

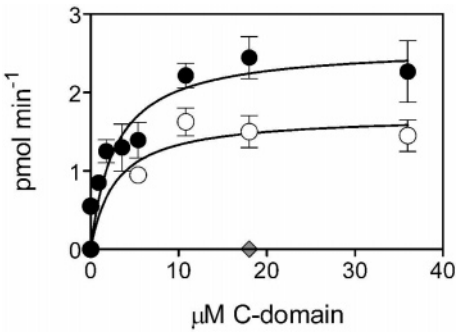

FIGURE 10: APS reductase activity of PaAPR with the EiAPR C domain as the electron donor. The C domain was titrated into a reaction with (●) 0.23 μM (0.8 μg) PaAPR, (○) 0.12 μM (0.4 μg) PaAPR, or (◇) no PaAPR. The reactions were carried out using GSH, GR, and NADPH as the reductant system and with 500 mM Na_2SO_4 added. Each data point represents the mean of at least three independent measurements. For those points without visible error bars, the standard deviation was less than the diameter of the line symbol.

Table 3: HED Reductase Activity

enzyme	μmol min^{-1} (mg of protein)$^{-1}$
Grx	5.7
C domain	9.5
EiAPR	0.6
hAPR	1.7
PaAPR	0

Table 4: Ribonucleotide Reductase Activity[a]

electron donor	activity (nmol min^{-1})
Trx	9.45
Grx	4.00
C domain	0.33

[a] All of the reactions contained 0.1 μM ribonucleotide reductase. The electron donors were 15 μM Trx, 8 μM Grx, or 70 μM C domain. Trx was used in combination with TR and NADPH, whereas Grx and C domain were used in combination with GR and NADPH. Each value is the mean of two independent measurements.

Although the C domain is very active in HED reduction, an activity typical of Grx, this may not be directly comparable to the APS reductase reaction observed in Figure 10. HED is a small metabolite and, unlike the case for PaAPR, HED reduction by the C domain would not be expected to require highly specific interactions of the sort found in electron transfer between proteins. Bick et al. (*14*) showed that the C domain of the APS reductase from *A. thaliana*, a typical plant-type enzyme, was capable of transferring electrons to *E. coli* ribonucleotide reductase, another reaction diagnostic for Grx-like behavior (*33*). The EiAPR C domain, which shows sequence homology to the C domain of the APS reductase from *A. thaliana*, was analyzed in the same way to ascertain how well it functions as an electron-transfer cofactor for a reductase. Table 4 and Figure 11 show that the free C domain is active as an electron donor for ribonucleotide reductase. However, its activity at the saturating concentration of the electron donor was only 4% of the activity with Trx and 8% of the activity with Grx (Table 3), demonstrating that the free C domain is a less active electron donor for ribonucleotide reductase than are Trx and Grx.

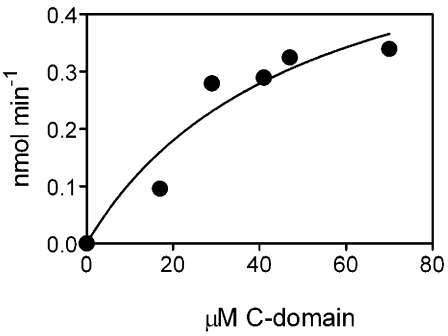

FIGURE 11: Ribonucleotide reductase activity using the C domain as the electron donor. The C domain was titrated into a ribonucleotide reductase assay. The reaction used 0.1 μM ribonucleotide reductase. Each data point is the mean of two independent measurements.

This finding was further emphasized by comparing the K_m values for the various electron donors used. The apparent K_m value for the C domain was found to be 49 μM (Figure 11). By comparison, the K_m values of 1.25 μM for Trx and 0.15 μM for Grx have been reported for the ribonucleotide-reductase-catalyzed reaction (*33*). The comparison shows that, although the C domain is highly active in HED reduction, it is not very active in donating electrons to protein partners. This may be due to the lack of specific regions involved in protein interactions on the C domain, perhaps because the primary mode for interacting with the reductase domain depends upon the presence of the two domains on the same polypeptide. However, the possibility that some aspect of the engineering required to express the C domain as a free protein may have interfered with its ability to interact with protein partners cannot be ruled out.

DISCUSSION

In this paper, evidence is presented that the physical linkage between the C domain of EiAPR and a heterologous enzyme (PaAPR) in hAPR provides the means by which the two proteins interact to produce GSH-dependent APS reductase activity. Furthermore, the result with the heterologous system suggests that the physical linkage may determine the interaction of domains in native plant APS reductases. This hypothesis was put forward by Bick et al. (*14*), who found that separation of the reductase domain from the C domain of *Arabidopsis* APR1 significantly reduced the catalytic efficiency of the enzyme and that none of several different Trx and Grx proteins, including the free C domain, was able to donate electrons efficiently to the free reductase. Although we did not rule out in this instance that the His tag at the amino terminus of the free C domain somehow interferes with its ability to interact with other enzymes (e.g., PaAPR), in a previous study, removal of the His tag did not affect the catalytic properties of the C domain of APR1 (*14*).

A second line of evidence that the physical association of PaAPR and C domain mimics the interaction of domains in native plant APS reductase is the finding that the activity of hAPR is stimulated by the addition of high concentrations of Na_2SO_4 to the reaction buffer. Stimulation by Na_2SO_4 is also a well-characterized property of plant APS reductases (*9*, *22*, *23*), having first been demonstrated in 1975, shortly after the discovery of this enzyme (in the initial literature, the enzyme was named APS sulfotransferase). By way of

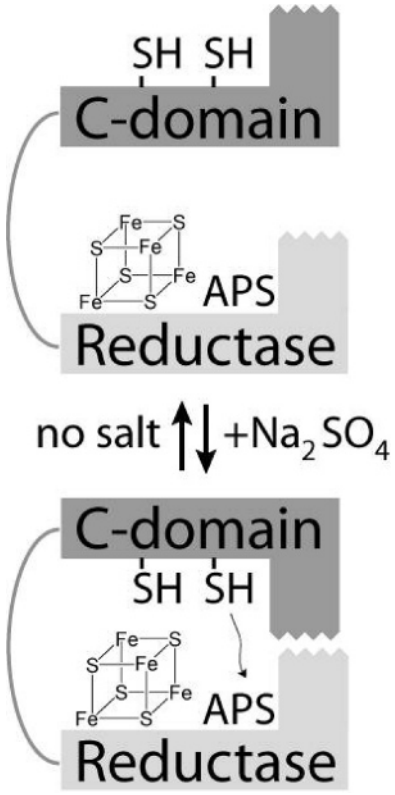

FIGURE 12: Model for the interaction of reductase and C domains, (top) without Na_2SO_4 and (bottom) with Na_2SO_4. The structure of the APS reductase is depicted as two independent domains connected by a linker sequence. When the active sites of the domains are positioned distally, the enzyme is in an inactive conformation (top diagram). When the active sites are located proximally, they are able to interact and the enzyme is in an active conformation. The interaction of domains is depicted as jagged lines representing hydrophobic domains. The active site of the reductase domain is depicted as APS bound to the $[4Fe-4S]^{2+}$ cluster of the enzyme. The nature of the active site is currently not known with certainty and might well include a Cys-sulfonate during part of the catalytic cycle (*5*, *17*).

an explanation, Schmidt (*23*) was the first to propose that a high ionic strength may stabilize the active conformation, although he was unaware of the bidomain structure, which was discovered in 1996 (*9*, *10*). The fact that the activity of PaAPR (*4*) and other bacterial APS reductases (personal observation by T.L.) are not stimulated by Na_2SO_4 but all plant APS reductases that have been studied are stimulated by Na_2SO_4 further suggests that the Na_2SO_4 requirement correlates with the bidomain structure. Interestingly, there appears to be a difference in the degree to which plant APS reductases respond to Na_2SO_4. For example, *Arabidopsis* APR1 is nearly inactive in the absence of Na_2SO_4 (*9*), but the activity of the orthologue APR2 is stimulated approximately 5-fold by Na_2SO_4 (as is EiAPR). The divergence in primary structure between these enzymes likely accounts for the difference. Na_2SO_4 is known to be a kosmotropic agent that is capable of organizing the structure of water around enzymes, thereby stabilizing hydrophobic domains. Indeed, it is for this property that Na_2SO_4 is commonly used in hydrophobic interaction chromatography (*32*). It is tempting to speculate that the interaction of domains in plant APS reductase is enhanced when weak hydrophobic interactions between the domains are stabilized. Figure 12 shows a model depicting the hypothesis that the active sites of the C domain

and reductase domain are positioned in an active conformation only when Na_2SO_4 is present and hydrophobic areas of the two domains interact. However, other mechanisms for the interaction of domains are also possible. The fact that not all kosmotropes are as efficient as Na_2SO_4 in stimulating activity suggests that salt-specific effects may play a role.

Other data in the paper are also of significance in confirming previously proposed properties of bacterial and plant APS reductases. The ability of the EiAPR C domain to confer GSH dependence onto PaAPR, an enzyme that by itself does not have the ability to use GSH, confirms that the C domain of EiAPR is the domain in plant APS reductases that interacts with GSH, consistent with the findings with *Arabidopsis* APR1 (*14*). Second, EiAPR was previously shown to contain two disulfide/dithiol couples that could be observed in oxidation−reduction titrations (*13*). The more positive couple was assigned to Cys residues in the C domain, and by deduction, the more negative couple was assigned to Cys residues in the reductase domain. In contrast, PaAPR was found to have a single disulfide/dithiol couple analogous to the more negative redox couple in EiAPR. The current evidence with hAPR confirms the assignments and further indicates that the engineered protein fusion did not disrupt the activity of the redox-active Cys residues.

ACKNOWLEDGMENT

The authors are grateful to Dr. Joanne Stubbe for providing ribonucleotide reductase.

NOTE ADDED IN PROOF

The structure of PaAPR was recently reported in *J. Mol. Biol. 364*, 152−169.

REFERENCES

1. Berendt, U., Haverkamp, T., Prior, A., and Schwenn, J. D. (1995) Reaction mechanism of thioredoxin: 3′-Phospho-adenylylsulfate reductase investigated by site-directed mutagenesis, *Eur. J. Biochem. 233*, 347−356.
2. Koprivova, A., Meyer, A. J., Schween, G., Herschbach, C., Reski, R., and Kopriva, S. (2002) Functional knockout of the adenosine 5′-phosphosulfate reductase gene in *Physcomitrella patens* revives an old route of sulfate assimilation, *J. Biol. Chem. 277*, 32195−32201.
3. Lillig, C. H., Prior, A., Schwenn, J. D., Aslund, F., Ritz, D., Vlamis-Gardikas, A., and Holmgren, A. (1999) New thioredoxins and glutaredoxins as electron donors of 3′-phosphoadenylylsulfate reductase, *J. Biol. Chem. 274*, 7695−7698.
4. Bick, J. A., Dennis, J. J., Zylstra, G. J., Nowack, J., and Leustek, T. (2000) Identification of a new class of 5′-adenylylsulfate (APS) reductases from sulfate-assimilating bacteria, *J. Bacteriol. 182*, 135−142.
5. Carroll, K. S., Gao, H., Chen, H., Stout, C. D., Leary, J. A., and Bertozzi, C. R. (2005) A conserved mechanism for sulfonucleotide reduction, *PLoS Biol. 3*, e250.
6. Kim, S. K., Rahman, A., Bick, J. A., Conover, R. C., Johnson, M. K., Mason, J. T., Hirasawa, M., Leustek, T., and Knaff, D. B. (2004) Properties of the cysteine residues and iron−sulfur cluster of the assimilatory 5′-adenylyl sulfate reductase from *Pseudomonas aeruginosa*, *Biochemistry 43*, 13478−13486.
7. Kopriva, S., Buchert, T., Fritz, G., Suter, M., Benda, R., Schunemann, V., Koprivova, A., Schurmann, P., Trautwein, A. X., Kroneck, P. M., and Brunold, C. (2002) The presence of an iron−sulfur cluster in adenosine 5′-phosphosulfate reductase separates organisms utilizing adenosine 5′-phosphosulfate and phosphoadenosine 5′-phosphosulfate for sulfate assimilation, *J. Biol. Chem. 277*, 21786−21791.
8. Berndt, C., Lillig, C. H., Wollenberg, M., Bill, E., Mansilla, M. C., de Mendoza, D., Seidler, A., and Schwenn, J. D. (2004) Characterization and reconstitution of a 4Fe−4S adenylyl sulfate/phosphoadenylyl sulfate reductase from *Bacillus subtilis*, *J. Biol. Chem. 279*, 7850−7855.
9. Setya, A., Murillo, M., and Leustek, T. (1996) Sulfate reduction in higher plants: Molecular evidence for a novel 5′-adenylylsulfate reductase, *Proc. Natl. Acad. Sci. U.S.A. 93*, 13383−13388.
10. Gutierrez-Marcos, J. F., Roberts, M. A., Campbell, E. I., and Wray, J. L. (1996) Three members of a novel small gene-family from *Arabidopsis thaliana* able to complement functionally an *Escherichia coli* mutant defective in PAPS reductase activity encode proteins with a thioredoxin-like domain and "APS reductase" activity, *Proc. Natl. Acad. Sci. U.S.A. 93*, 13377−13382.
11. Kopriva, S., Buchert, T., Fritz, G., Suter, M., Weber, M., Benda, R., Schaller, J., Feller, U., Schurmann, P., Schunemann, V., Trautwein, A. X., Kroneck, P. M., and Brunold, C. (2001) Plant adenosine 5′-phosphosulfate reductase is a novel iron−sulfur protein, *J. Biol. Chem. 276*, 42881−42886.
12. Gao, Y., Schofield, O. M., and Leustek, T. (2000) Characterization of sulfate assimilation in marine algae focusing on the enzyme 5′-adenylylsulfate reductase, *Plant Physiol. 123*, 1087−1096.
13. Kim, S. K., Rahman, A., Conover, R. C., Johnson, M. K., Mason, J. T., Gomes, V., Hirasawa, M., Moore, M. L., Leustek, T., and Knaff, D. B. (2006) Properties of the cysteine residues and the iron−sulfur cluster of the assimilatory 5′-adenylyl sulfate reductase from *Enteromorpha intestinalis*, *Biochemistry 45*, 5010−5018.
14. Bick, J. A., Aslund, F., Chen, Y., and Leustek, T. (1998) Glutaredoxin function for the carboxyl-terminal domain of the plant-type 5′-adenylylsulfate reductase, *Proc. Natl. Acad. Sci. U.S.A. 95*, 8404−8409.
15. Carroll, K. S., Gao, H., Chen, H., Leary, J. A., and Bertozzi, C. R. (2005) Investigation of the iron−sulfur cluster in *Mycobacterium tuberculosis* APS reductase: Implications for substrate binding and catalysis, *Biochemistry 44*, 14647−14657.
16. Kim, S. K., Rahman, A., Mason, J. T., Hirasawa, M., Conover, R. C., Johnson, M. K., Miginiac-Maslow, M., Keryer, E., Knaff, D. B., and Leustek, T. (2005) The interaction of 5′-adenylylsulfate reductase from *Pseudomonas aeruginosa* with its substrates, *Biochim. Biophys. Acta 1710*, 103−112.
17. Weber, M., Suter, M., Brunold, C., and Kopriva, S. (2000) Sulfate assimilation in higher plants characterization of a stable intermediate in the adenosine 5′-phosphosulfate reductase reaction, *Eur. J. Biochem. 267*, 3647−3653.
18. Sun, Q. A., Su, D., Novoselov, S. V., Carlson, B. A., Hatfield, D. L., and Gladyshev, V. N. (2005) Reaction mechanism and regulation of mammalian thioredoxin/glutathione reductase, *Biochemistry 44*, 14528−14537.
19. Rouhier, N., Gama, F., Wingsle, G., Gelhaye, E., Gans, P., and Jacquot, J.-P. (2006) Engineering functional artificial hybrid proteins between poplar peroxiredoxin II and glutaredoxin or thioredoxin, *Biochem. Biophys. Res. Commun. 341*, 1300.
20. Li, X., Nield, J., Hayman, D., and Langridge, P. (1995) Thioredoxin activity in the C terminus of *Phalaris* S protein, *Plant J. 8*, 133−138.
21. Prior, A., Uhrig, J. F., Heins, L., Wiesmann, A., Lillig, C. H., Stoltze, C., Soll, J., and Schwenn, J. D. (1999) Structural and kinetic properties of adenylyl sulfate reductase from *Catharanthus roseus* cell cultures, *Biochim. Biophys. Acta 1430*, 25−38.
22. Kanno, N., Nagahisa, E., Sato, M., and Sato, Y. (1996) Adenosine 5′-phosphosulfate sulfotransferase from the marine macroalga *Porphyra yezoensis* Ueda (*Rhodophyta*)—Stabilization, purification, and properties, *Planta 198*, 440−446.
23. Schmidt, A. (1975) A sulfotransferase from spinach leaves using adenosine-5′-phosphosulfate, *Planta 124*, 267−275.
24. Bradford, M. M. (1976) A rapid and sensitive method for the quantitation of microgram quantities of protein utilizing the principle of protein−dye binding, *Anal. Biochem. 72*, 248−254.
25. Krimm, I., Lemaire, S., Ruelland, E., Miginiac-Maslow, M., Jaquot, J. P., Hirasawa, M., Knaff, D. B., and Lancelin, J. M. (1998) The single mutation Trp35 → Ala in the 35−40 redox site of *Chlamydomonas reinhardtii* thioredoxin *h* affects its biochemical activity and the pH dependence of C36−C39 ^{1}H-^{13}C NMR, *Eur. J. Biochem. 255*, 185−195.
26. Hirasawa, M., Schurmann, P., Jacquot, J. P., Manieri, W., Jacquot, P., Keryer, E., Hartman, F. C., and Knaff, D. B. (1999) Oxidation−reduction properties of chloroplast thioredoxins, ferredoxin: thioredoxin reductase, and thioredoxin *f*-regulated enzymes, *Biochemistry 38*, 5200−5205.

27. Setterdahl, A. T., Goldman, B. S., Hirasawa, M., Jacquot, P., Smith, A. J., Kranz, R. G., and Knaff, D. B. (2000) Oxidation-reduction properties of disulfide-containing proteins of the *Rhodobacter capsulatus* cytochrome *c* biogenesis system, *Biochemistry 39*, 10172−10176.
28. Massey, V. (1957) Studies on succinic dehydrogenase. VII. Valency state of the iron in beef heart succinic dehydrogenase, *J. Biol. Chem. 229*, 763−770.
29. King, T. E., and Morris, R. O. (1967) Determination of acid-labile sulfide and sulfhydryl groups, *Methods Enzymol. 10*, 634−641.
30. Czernuszewicz, R. S., Macor, K. A., Johnson, M. K., Gewirth, A., and Spiro, T. G. (1987) Vibrational mode structure and symmetry in proteins and analogs containing Fe_4S_4 clusters: Resonance Raman evidence for different degrees of distortion in HiPIP and ferredoxin, *J. Am. Chem. Soc. 109*, 7178−7187.
31. Bick, J. A., Setterdahl, A. T., Knaff, D. B., Chen, Y., Pitcher, L. H., Zilinskas, B. A., and Leustek, T. (2001) Regulation of theplant-type 5′-adenylyl sulfate reductase by oxidative stress, *Biochemistry 40*, 9040−9048.
32. Melander, W. R., Corradini, D., and Horvath, C. (1984) Salt-mediated retention of proteins in hydrophobic-interaction chromatography. Application of solvophobic theory, *J. Chromatogr. 317*, 67−85.
33. Holmgren, A. (1979) Glutathione-dependent synthesis of deoxyribonucleotides. Characterization of the enzymatic mechanism of *Escherichia coli* glutaredoxin, *J. Biol. Chem. 254*, 3672−3678.

BI0618971